Published online 4 December 2009

Nucleic Acids Research, 2010, Vol. 38, No. 4 ***e24***
doi:10.1093/nar/gkp1082

Analysis of differential DNA damage in the mitochondrial genome employing a semi-long run real-time PCR approach

Oliver Rothfuss[1,2], Thomas Gasser[1] and Nadja Patenge[1,*]

[1]Center for Neurology and Hertie Institute for Clinical Brain Research, Department of Neurodegeneration, University of Tuebingen, 72076 Tuebingen and [2]Graduate Training Centre of Neuroscience, International Max Planck Research School, University Tübingen, 72074 Tübingen, Germany

Received June 22, 2009; Revised November 4, 2009; Accepted November 5, 2009

ABSTRACT

The maintenance of the mitochondrial genomic integrity is a prerequisite for proper mitochondrial function. Due to the high concentration of reactive oxygen species (ROS) generated by the oxidative phosphorylation pathway, the mitochondrial genome is highly exposed to oxidative stress leading to mitochondrial DNA injury. Accordingly, mitochondrial DNA damage was shown to be associated with ageing as well as with numerous human diseases including neurodegenerative disorders and cancer. To date, several methods have been described to detect damaged mitochondrial DNA, but those techniques are semi-quantitative and often require high amounts of genomic input DNA. We developed a rapid and quantitative method to evaluate the relative levels of damage in mitochondrial DNA by using the real time-PCR amplification of mitochondrial DNA fragments of different lengths. We investigated mitochondrial DNA damage in SH-SY5Y human neuroblastoma cells exposed to hydrogen peroxide or stressed by overexpression of the tyrosinase gene. In the past, there has been speculation about a variable vulnerability to oxidative stress along the mitochondrial genome. Our results indicate the existence of at least one mitochondrial DNA hot spot, namely the D-Loop, being more prone to ROS-derived damage.

INTRODUCTION

Mitochondria are responsible for maintaining the cellular energy balance and are involved in the triggering of apoptosis in response to oxidative stress. The majority of mitochondrial proteins is encoded by nuclear DNA. Nevertheless, mitochondria harbour their own genome consisting of a circular duplex molecule of approximately 16.5 kb encoding 13 polypeptides that are exclusively involved in the intracellular ATP production by the electron transport chain (ETC) as well as two rRNAs and 22 tRNAs essential for mitochondrial polypeptide synthesis (1). Like the mitochondrial DNA (mtDNA), the ETC is localized at the inner side of the mitochondrial inner membrane. The ETC reduces oxygen to water in four consecutive one-electron steps. As a by-product of this process, reactive oxygen species (ROS) are produced. These reactive molecules can be converted to H_2O_2 spontaneously or by superoxide dismutase culminating in free hydroxyl radicals (•OH) via Fenton chemistry (2). ROS, in particular hydroxyl radicals, exhibit a high capacity to impair proteins, lipid membranes, DNA and RNA, which are essential components of functional mitochondria.

Due to the high reactive environment, and probably due to a mitochondrial chromatin-like structure condensed to a lesser extent than nuclear chromatin, the mtDNA is frequently exposed to oxidative stress leading to mitochondrial genomic defects (3,4). The most prevalent forms of mtDNA mutations are point mutations, nucleic acid modifications and large-scale deletions, all of which culminate in mitochondrial dysfunction and apoptosis (5–7). Consequently, mtDNA damage was shown to be associated with ageing (8) and numerous human diseases such as cancer (9–11) and neurodegenerative disorders like Alzheimer (12–14), Parkinson (5,14–16), Huntington disease (17,18) and amyotrophic lateral sclerosis (19,20). Thus, mtDNA damage, as a result of environmental insults or enhanced by genetic predisposition, attracts increasingly attention as the origin of mitochondrial dysfunction.

In the last decade, numerous discoveries were made on DNA repair in the mitochondria and the base excision

*To whom correspondence should be addressed. Tel: +49 381 4945939; Fax: +49 381 4945902; Email: nadja.patenge@med.uni-rostock.de
Present address:
Institute of Medical Microbiology, Virology and Hygiene, University of Rostock, Schillingallee 70, 18057 Rostock, Germany.

repair pathway was identified as the major mtDNA repair mechanism (1,10,21). However, only a limited number of molecular biological and analytical methods is available to detect damaged DNA caused by genotoxic insults.

Recently, Santos and co-workers established a long-run quantitative PCR method that permits the amplification of up to 25 kb genomic DNA fragments using as little as several nanogram of total DNA (22). Although this long-run PCR clearly facilitates nuclear and mitochondrial DNA damage determination, the multi-step procedure is still time-consuming, and requires a high degree of optimization and accuracy for reliable experimental results. More recently, this method was further modified by the use of a high processivity polymerase applicable for real-time amplification of fragments covering nearly the entire mitochondrial genome (23).

Here, we describe a novel rapid, gene-specific and simplified semi-long run real-time (SLR rt-) PCR method for the accurate quantification of mtDNA lesions induced by oxidative stress that can be implemented within less than three hours. In contrast to long run approaches, amplicon sizes up to 1000 bp for the determination of DNA lesions allow the investigation of mtDNA vulnerability in small, well-defined regions along the mitochondrial genome. This rt-PCR based application detects DNA variations that interfere with the polymerase-based DNA amplification. Common ROS-derived DNA damage products include strand breaks, base modifications and bulky DNA adduct formation either inhibiting primer annealing or blocking the polymerase driven synthesis of the complementary DNA strand (24). As a matter of principle, in rt-PCR analysis, in contrast to endpoint PCR approaches, no extensive adjustment of DNA template concentration is necessary for accurate DNA quantification and thus for an efficient and quick DNA damage determination. The timing chart of the entire damage assay is displayed in Figure 1A. Employing a cell culture model stressed with a chemical insult, we were able to show a concentration-dependent increase of mtDNA damage. Comparing several independent regions evenly distributed along the mitochondrial genome, we found the level of lesions induced by H_2O_2 exclusively increased in the fragment harbouring the regulatory D-Loop. Moreover, we were able to monitor mtDNA recovery following H_2O_2 incubation. In summary, our protocol provides for the first time the means to study the vulnerability of specific mtDNA regions to damaging agents and the mtDNA recovery efficiency under these conditions. The method is quick, accurate, and easy to control for experimental parameters. These characteristics make it interesting for researchers from different fields, who aim for studying the effects of mtDNA damage on cellular function and its influence on the pathogenesis of a variety of diseases.

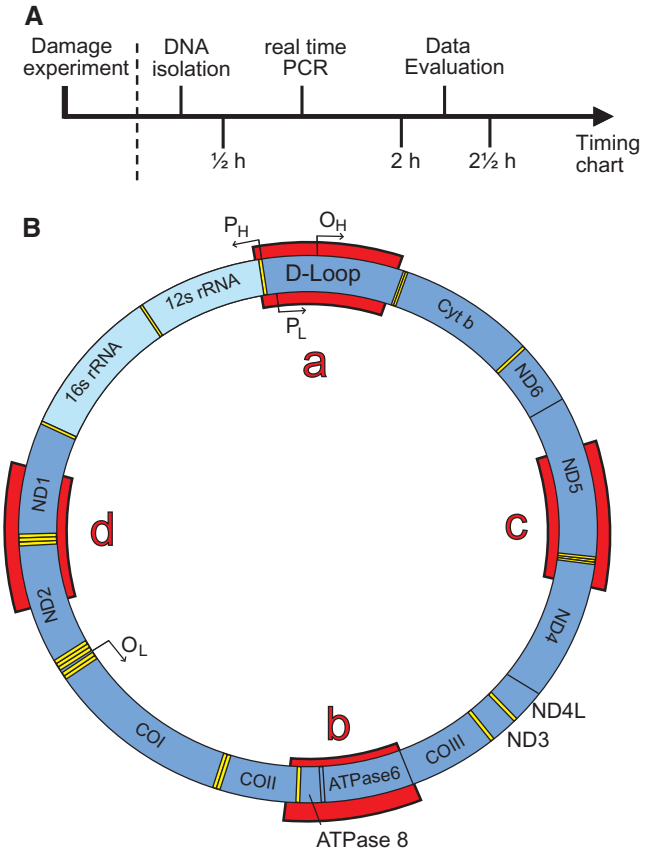

Figure 1. Primer selection and Timing Chart. The experimental flow-chart of the SLR rt-PCR method (**A**). A schematic view of the mitochondrial genome (**B**). The four selected 1 kb sized regions [red sectors a–d; mtDNA position: chrM:16021 + 423 (a); chrM:8204 + 9203 (b); chrM:12050 + 13049 (c); chrM:3962 + 4998 (d)] were employed for the SLR rt-PCR approach to quantify the MLF. Mitochondrial genes are almost introns-less arranged on both strands (heavy and light) and code for 22 transfer RNAs (yellow bars), the small and large subunits of ribosomal RNA (bright blue curved squares) and 13 proteins implicated in the oxidative phosphorylation (dark blue). O_H, replication origin for heavy strand; O_L, replication origin for light strand; P_L, light strand promoter; P_H, heavy strand promoter.

MATERIAL AND METHODS

Cell culture and DNA damage assay

The catecholaminergic SH-SY5Y neuroblastoma cell line originated from ATCC (#CRL-2266) was grown in Dulbecco's modified Eagle's medium DMEM/HAM F12 (Biochrome, Germany) and 10% heat-inactivated Foetal Bovine Serum (PAA Laboratories, Austria). For ROS-induced mtDNA damage generation, cells were exposed to hydrogen peroxide (H_2O_2) (Sigma-Aldrich, Germany) in serum-free media for 0.5 h as indicated. H_2O_2 was removed by two times washing with standard culture media. Cells were harvested immediately or allowed to repair for indicated time points.

Stably expressing human tyrosinase SH-SY5Y cells (TR8/TY) were cultured in Dulbecco's modified Eagle's medium (Biochrome, Germany) supplemented with 10% fetal bovine serum (PAA Laboratories, Austria) and 2 mM L-glutamine (Invitrogen) at 37°C under 5% CO_2/air including selection media containing 7 µg/ml blasticidin (InvivoGen, San Diego, CA, USA) for pcDNA6/TR and 300 µg/ml Zeocin (InvivoGen) for pcDNA4/tyrosinase as previously described (25).

Induction of human tyrosinase expression was achieved by the addition of 1 μg/μl doxycycline (MP Biomedials, Solon, OH, USA). In both cellular models oxidative stress derived cytotoxcity was monitored by the LDH release assay as described (26).

DNA isolation and purification

Total DNA was purified using DNA Blood and Tissue Kit (Qiagen, Germany) from cells under standard and under ROS generating conditions, respectively, and DNA quantity and purity was determined by spectrometric analysis. The isolated DNA showed a high purity ($A_{260}/A_{280} > 1.8$) and was stored at 4°C according to standard procedures.

Oligonucleotides

All Primers for the real-time applications (rt) were designed using Primer 3 software, synthesized and HPLC-purified by Metabion international, Germany. The sequence of all primers used in this study can be found in Table 1.

Semi-long run rt-PCR

The SLR rt-PCR amplifications were conducted in the Light Cycler 2.0 system (Roche, Germany), and the amplification was monitored and analysed by measuring the intercalation of the fluorescent dye to double-stranded DNA supplied by the Fast Start DNA Master plus SYBR Green I kit (Roche, Germany) according to the manufacturer's instructions. To compare the levels of DNA lesion in each tested region of the mitochondrial genome, two mtDNA fragments of different lengths (long fragments ranging from 972 to 1037 bp and small fragments from 54 to 87 bp, respectively), located in the same mitochondrial genomic region were used. The mtDNA regions selected for rt-PCR are displayed in Figure 1B. The HPLC-purified oligonucleotides used in this study, the PCR settings, and their PCR efficiencies are listed in Table 1.

The PCR conditions for the different fragments were optimized to achieve similar amplification efficiencies required to compare different amplicons. The product specificity was monitored by melting curve analysis and product size was visualized on agarose gel by electrophoresis (data not shown). The reaction mix (total volume $V = 10$ μl) consists of 1 × SYRB Green Master mix, 500 nM each forward and reverse primer (specific for the long or the short amplicon, respectively) and the equivalent quantities of template DNA (3 ng of total DNA). The cycling conditions include a pre-incubation phase of 10 min at 95°C followed by 40 cycles of 10 s 95°C, 10 s 60°C, and 10 s 72°C (small fragments) or 50 s 72°C (large fragments), respectively. Each sample was assayed in quadruplicate, fluorescence was continuously monitored versus cycle numbers and crossing point values were calculated by the Light Cycler 3 software version 3.5 (Roche).

To compare the DNA damage rate in our experimental system generated by the SLR rt-PCR method with an already established PCR-based approach, we conducted the quantitative PCR method from Santos and colleagues (22) employing the 8,9 kb DNA fragment as previously described.

rt–PCR data analysis

Data analysis is based on the measurement of the crossing point (C_p). Isolated total DNA from untreated sample was taken as reference. For each of the four mtDNA regions the difference in the crossing point ΔC_p (long fragment/small fragment) was used as a measure of the relative MLF with the $2^{-\Delta\Delta CT}$ method in correlation to the amplification size of the long fragment (27).

Briefly, for the quantification of damage in each mtDNA region, rt-PCR analysis for the corresponding small and long fragments was performed consecutively. For each experimental condition rt-PCR was conducted in quadruplicates and the resulting average of C_p values for the long and the small fragment were used for the evaluation of DNA damage quantity. Therefore, the

Table 1. Oligonucleotides and their SLR rt-PCR parameter used in this study

Primer	Sequence	Size (bp)	Template	T_{an} (°C)	t_{elong} (s)	PCR efficiency (%)
AS1.F	CCCTAACACCAGCCTAACCA	55	chrM:369 + 423		10	98.2
AS1.R	AAAGTGCATACCGCCAAAAG					
BS1.F	CATGCCCATCGTCCTAGAAT	54	chrM:8204 + 8257		10	97.2
BS1.R	ACGGGCCCTATTTCAAAGAT					
CS1.F	TCCAACTCATGAGACCCACA	55	chrM:12914 + 12968		10	99.9
CS1.R	TGAGGCTTGGATTAGCGTTT					
DS1.F	ACTACAACCCTTCGCTGACG	87	chrM:3442 + 3528		10	99.7
DS1.R	GCGGTGATGTAGAGGGTGAT			60		
AL4.F	CTGTTCTTTCATGGGGAAGC	972	chrM:16021 + 423		50	69.4
AS1.R	AAAGTGCATACCGCCAAAAG					
BL1.F	CATGCCCATCGTCCTAGAAT	1000	chrM:8204 + 9203		50	89.0
BL1.R	TGTTGTCGTGCAGGTAGAGG					
CL1.F	CACACGAGAAAACACCCTCA	1000	chrM:12050 + 13049		50	85.1
CL1.R	CTATGGCTGAGGGGAGTCAG					
DL1.F	CCCTTCGCCCTATTCTTCAT	1037	chrM:3962 + 4998		50	85.4
DL1.R	GCGTAGCTGGGTTTGGTTTA					

difference in the crossing point ΔC_p of untreated versus each treated condition of the respective long and small fragments was calculated by the $2^{-\Delta\Delta CT}$ method expressed as ratio of intact DNA. The DNA damage was calculated as lesion per 10 kb DNA of each mtDNA region by including the size of the respective long fragment and displayed as average of at least three independent experiments.

$$\text{Lesion rate [Lesion per 10 kb DNA]} = \left(1 - 2^{-(\Delta_{long} - \Delta_{short})}\right) \times \frac{10000\,[\text{bp}]}{\text{size of long fragment [bp]}}. \quad (1)$$

Determination of mitochondrial copy number

Quantitative rt-PCR was carried out as described above by amplifying equal amounts of total DNA isolated from differentially treated cells using genomic primers for mitochondrial sequences: BS1 (54 bp fragment size) and ChIP9 (157 bp fragment size) forward 5′-CACCTACCT CCCTCACCAAA-3′, reverse 5′-GGGATCAATAGAG GGGGAAA-3′, respectively. The experiments were performed at least on three independent occasions and each sample was assayed in quadruplicate. Nuclear DNA sequences LC3 (220 bp fragment size), forward 5′-GTGA ATTGGGCTGTGAGTGT-3′, reverse 5′-AGCCAAAG GTGCATTTCGTA-3′ and ChIP14 (236 bp fragment size), forward 5′-GGTGCCTGGGAAGGATTAAA-3′, reverse 5′-TCTCAGCATACTTGAGGTTTCC-3′; and ChIP7.2 (176 bp fragment size) forward 5′-TGGGGGTG ACTTACAGAAGG-3′, reverse 5′-GGTTGAACTGCCA CTCACCT-3′) and non-treated cells were used as reference sample.

Statistical analysis

The data are presented as the means ± SE of three independent experiments unless stated otherwise.

RESULTS

Validation of the SLR rt-PCR assay

The basic principle of our method relies on the rt-PCR-based amplification rate of two mtDNA fragments of different length. Amplification of the bigger fragment serves as experimental probe to observe the level of lesions introduced by oxidative stress. The short product, an adjoining fragment of <90 bp, serves as internal normalization control. Under cellular and physiological relevant conditions, the amplification of short nucleotide sequences statistically represents undamaged mtDNA due to the low probability of lesion generation in small DNA fragments by a moderate ROS level (22). The mitochondrial lesion frequency (MLF) can be calculated by the ratio of lesion occurrence per amplified nucleotide size and normalized to DNA magnitude by assuming a Poisson distribution of randomly generated lesions along the mitochondrial genome (28). As a consequence, MLF is inversely proportional to the amplification depending on its sequence length.

To evaluate the levels of lesions induced by oxidative stress at different targets of the mitochondrial genome, we selected four experimental probes and respective internal controls for amplification, which are evenly distributed along the mtDNA. Three experimental sequences contained regions, which were located in the ND5, ND1/ND2 and COII/ATPase6/8 genes, respectively. In addition, one amplicon was situated in the D-Loop, which exhibits a triple-stranded, semi-stable DNA structure during replication (29,30). Due to its partially relaxed structure, we hypothesized that the D-Loop is more prone to oxidative damage than other mtDNA regions. Figure 1B displays a schematic representation of the mitochondrial DNA and the localisation of the four selected mitochondrial genomic regions analysed in this study.

To validate the SLR rt-PCR assay, total DNA was isolated from SH-SY5Y cells yielding similar DNA concentrations (c = 300 ng/µl) and logarithmically diluted 1 : 10 to 1 : 10 000, corresponding to ~30 ng to 30 pg of total DNA, and amplified using long-run rt-PCR with primers for all fragments (Figure 2A–H). To ensure an unbiased comparison of the amplification of the big and the small fragment of the same sample, the amplification efficiencies were calculated according to the equation $E = 10^{(-1/\text{slope})}$ (31) resulting in 97.2–99.9% for the fragments below 90 bp sizes and 69.4–89% for the 1 kb fragments, respectively (Table 1). The relationship between the C_p value and the logarithmic dilution values of total DNA was linear with correlation coefficients R^2 ranging from 0.9996 to 1 for all tested amplicons. As a result, the SLR rt-PCR assay shows a high linearity over a wide range of template concentrations which enables a consistent and precise determination of DNA damage within all tested DNA template quantities. Together these data show that all sequences are amplifiable with comparable efficiencies, which allows the investigation of mitochondrial DNA damage in an accurate and highly reliable fashion using the Semi Long Run rt-PCR with our settings.

The D-loop region is more vulnerable to ROS induced mtDNA damage

First, testing the sensitivity of mtDNA damage quantification using our SLR rt-PCR approach, we employed H_2O_2 treatment to induce oxidative damage. Therefore, neuroblastoma SH-SY5Y cells were exposed to hydrogen peroxide (H_2O_2, Sigma) for 0.5 h as indicated. H_2O_2 was removed by two-times washing with standard culture medium. The results of three independent DNA damage experiments by SLR rt-PCR analysis are shown in Figure 3A–D. Consistently, the SLR rt-PCR analysis revealed a similar lesion rate in all tested coding regions [ND1/2 (D), ND4/5 (C), and COII/ATPase6/8 (B)]. Initial DNA damage was observed in SH-SY5Y cells treated with 100 µM H_2O_2 yielding from 0.13 lesions per 10 kb DNA in the COII/ATPase 6/8 domain (B), and 0.14 lesions in the ND4/5 domain (C), to 0.29 lesions in the ND1/2 domain (D). In addition, a steady increase of mtDNA lesions is attended by an elevation of H_2O_2 concentration from

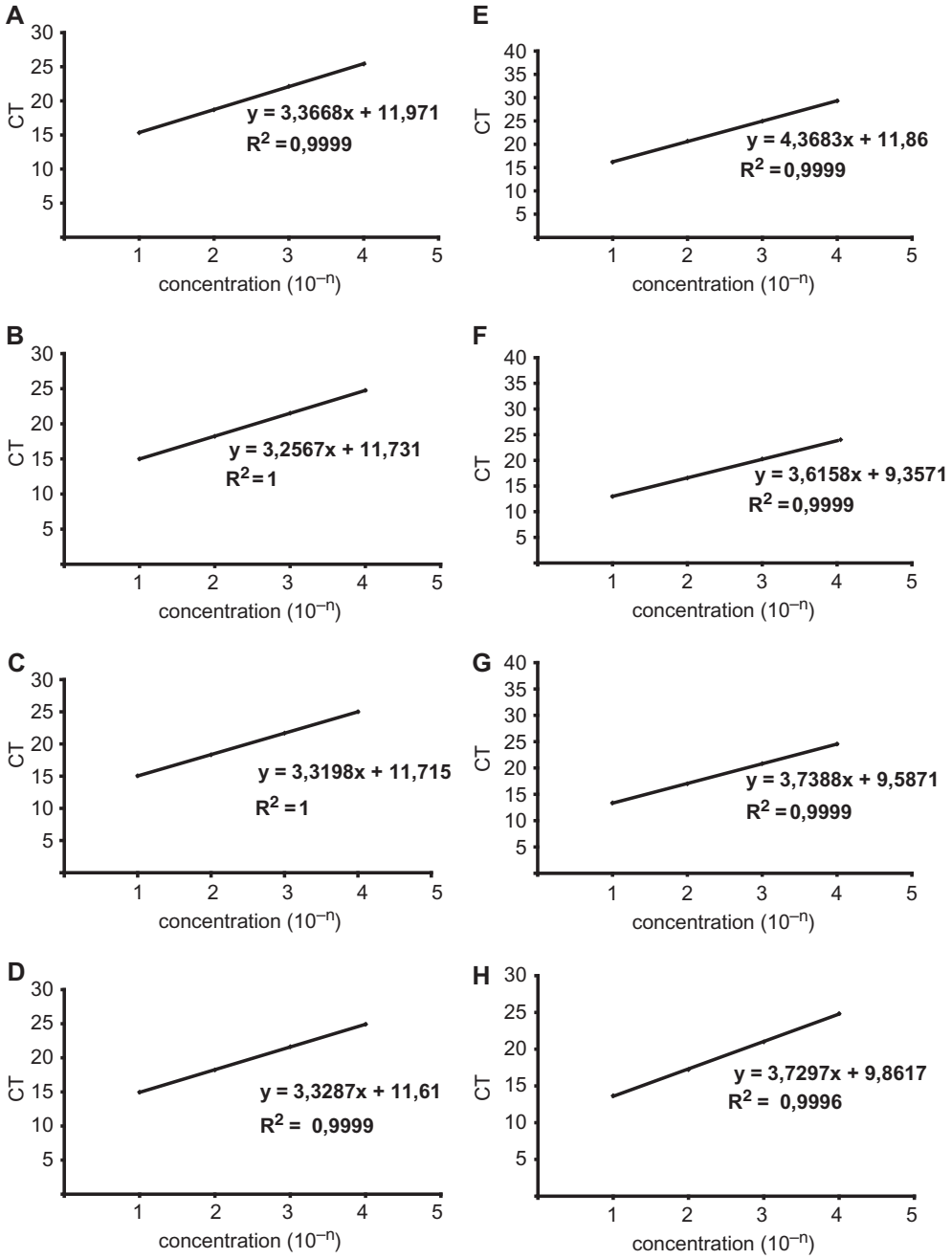

Figure 2. Characterization of real-time PCR. To test the validity of the mtDNA damage assay over a broad range of total DNA concentration, real-time amplification was performed (**A**) for the 55 bp fragment on chrM:369 + 423, (**B**) for the 54 bp fragment on chrM: 8204 + 8257, (**C**) for the 55 bp fragment on chrM: 12914 + 12968, (**D**) 87 for the 55 bp fragment on chrM:3442 + 3528, (**E**) for the 972 bp fragment on chrM:16021 + 423, (**F**) for the 1000 bp fragment on chrM:8204 + 9203, (**G**) for the 1000 bp fragment on chrM:12050 + 13049, (**H**) and for the 1037 bp fragment on chrM:3962 + 4998 over a range of 30 ng to 30 pg total DNA isolated from SH-SY5Y cells, respectively. The amplification resulted in an inverse linear relationship with the C_p values and the dilution of total DNA templates with correlation coefficients between 1 and 0.9996, respectively. MtDNA damage assay shows high linearity over a wide range of template concentration with comparable amplification efficiencies E from 97.2 to 99.9% for the fragments below 90 bp sizes and 69.4 to 89% for the 1 kb fragments, respectively.

100 μM to 1 mM. Strikingly, a 5-fold higher lesion rate was observed in the non-coding regulatory D-Loop (A) after treatment with 100 μM H_2O_2 resulting in 1.7 lesions per 10 kb DNA. The increase of lesion rate in the D-Loop versus tested coding regions was 4-fold (3.5 lesions per 10 kb DNA/0.85 lesions per 10 kb DNA) in cells treated with 200 μM and 2.5-fold (4.9/1.94) in cells treated with 500 μM H_2O_2, respectively. The difference of lesion rates between the non-coding regulatory D-Loop and the three coding regions was alleviated in templates treated with a high peroxide concentration (750 μM H_2O_2: D-Loop 5.9 lesions/10 kb DNA, coding regions 4.2–4.5 lesions/10 kb DNA; 1000 μM H_2O_2: D-Loop 6.1 lesions/10 kb DNA, coding regions 4.8–5.3

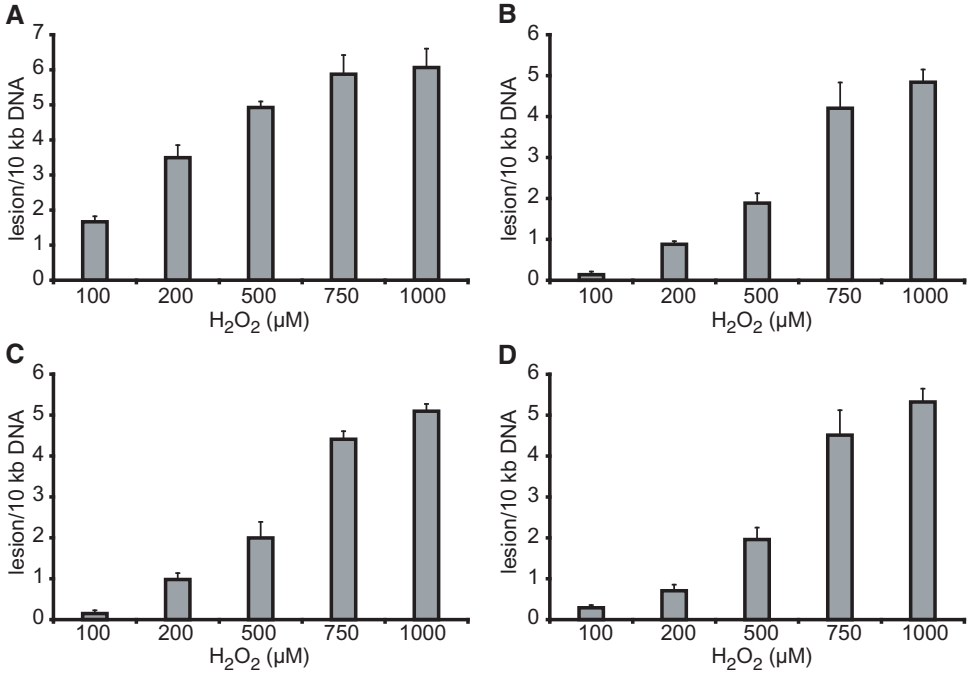

Figure 3. H_2O_2/ROS-induced mtDNA lesions. Quantification of mtDNA damage per 10 kb DNA by SLR rt-PCR amplification of total DNA isolated from SH-SY5Y cells exposed to 0–1000 μM hydrogen peroxide for 30 min showing an steadily increasing mtDNA damage over hydrogen peroxide concentration in all tested mtDNA regions. mtDNA damage was calculated using the Δ2Ct method and expressed as relative DNA lesion rate. By SLR rt-PCR, similar lesion rate were observed in all tested coding regions [COII/ATPase6/8 (B), ND4/5 (C), and ND1/2 (D)], whereas the D-Loop (A) exhibited increased mitochondrial lesion frequency (MLF). Error bars designate standard deviation (at least three independent experiments).

lesions/10 kb DNA). In parallel, oxidative stress derived cytotoxcity was measured by LDH release. In our experimental settings, low H_2O_2 concentrations (0–200 μM) caused minor cytotoxcity. LDH release increased steadily in a H_2O_2 concentration dependant manner as illustrated in Supplementary Figure S1. In addition, during the oxidative stress exposure the cells exhibited no obvious sign of severe cell disruption, morphological changes or cell displacement by microscopic observation.

To compare the sensitivity and accuracy of our experimental system with the method developed by Santos and colleagues (22), we conducted the quantitative PCR-based approach employing the 8.9 kb fragment described in their report. To ensure optimal experimental settings, we monitored the relative amplification of all sample templates and a 50% control template yielding to an acceptable relative amplification of 51% (Figure 4A). Employing the same experimental templates, no DNA damage was observed in the samples treated with 100 μM and 200 μM H_2O_2 (Figure 4B). Templates isolated from cells treated with elevated H_2O_2 concentrations (500–1000 μM) exhibited steadily increasing DNA damage quantities of 1.0 (500 μM), 2.2 (750 μM) and 3.4 lesions/10 kb DNA (1000 μM H_2O_2). In our hands, performance of this method led to large standard deviations. In summary, data obtained with our method are in the same range as the results achieved by employing the method of Santos and co-workers. However, we observed with our new method a higher sensitivity combined with very consistent and precise MLF scales. As a consequence of the sensitive rt-PCR methodology, biological relevant MLF of >1 lesion per 10 kb mtDNA can be detected, which enables the examination of physiological mtDNA damage and potential repair processes *in vivo*.

In a second approach, we wanted to test whether we were able to detect ROS derived mtDNA damage in a more physiological context than chemical insults. To that end, we performed the DNA damage assay with the TR8TY8 neuronal cell line generated by Hasegawa and co-workers, which exogenously expresses human tyrosinase in the presence of tetracycline. The induction of tryosinase expression leads to an increase of the intracellular dopamine content and, as a consequence of induced oxidase activity, finally increases the intracellular ROS level (25). We investigated the impact of tyrosinase expression on the generation of mtDNA lesions using the SLR rt-PCR approach. Following induction of tyrosinase expression, we harvested the cells and subsequently isolated total DNA at indicated time points. In this approach, the non induced cells served as reference and DNA damage was determined for all four mitochondrial genomic regions. Employing SLR rt-PCR analysis, initial DNA damage was detected at Day 3 with 2.0 lesions per 10 kb mtDNA increasing to 3.5 lesions at Day 4 and 4.8 lesions per 10 kb mtDNA at Day 5 in the COII/ATPase 6/8 domain (Figure 5A). Similar DNA damage rates were observed in the ND4/5 and ND1/2 coding

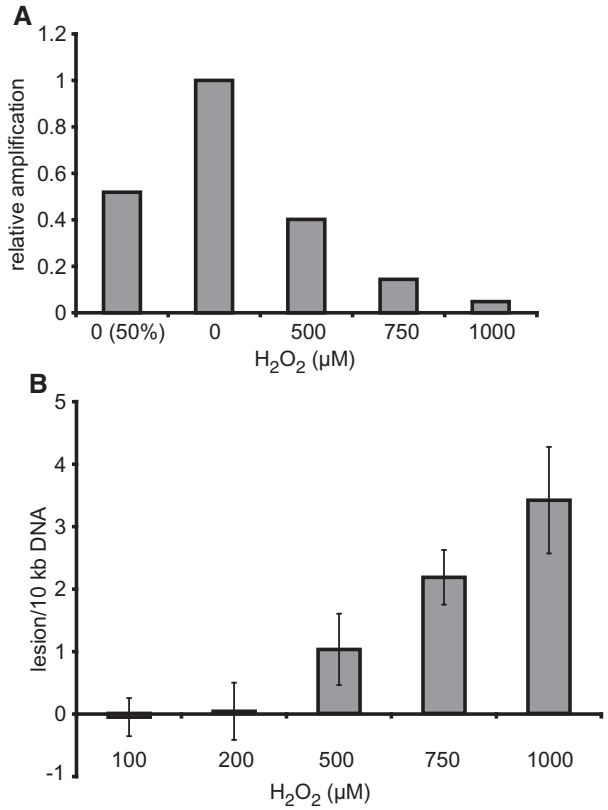

Figure 4. Quantitative measurement of mitochondrial DNA damage using the technique of Santos and co-workers (22). Representation of the relative amplification of the 8.9 kb mitochondrial fragment comparing the amplicon amounts of treated versus undamaged control (**A**). To monitor performance of an optimal QPCR procedure 50% of reference template was amplified resulting in 51% of relative amplification rate. Lesion frequencies of treated samples were calculated per amplicon size and expressed per 10 kb of mitochondrial genome (**B**).

regions (data not shown). Consistent with the H_2O_2 induced genomic damage approach, DNA lesion analysis of the non-coding D-loop region revealed an overall increased damage rate compared to the coding regions (COII/ATPase 6/8, ND4/5 and ND1/2). Detectable D-loop lesions initially occurred at Day 2 after tyrosinase induction (1.6 lesions/10 kb), and steadily elevated to 5.3 lesions per 10 kb mtDNA at Day 5 (Figure 5B). In summary, employing our method, we were able to detect increasing DNA damage correlating with the magnitude of oxidative stress in two different experimental models. Moreover, we were able to show enhanced vulnerability of the regulatory D-loop region towards oxidative stress in comparison to the coding regions of the mitochondrial genome.

mtDNA recovery kinetics upon ROS damage

We wanted to test whether our SLR rt-PCR assay is applicable to monitor the recovery of mtDNA following oxidative stress. In order to perform the assay, mtDNA lesions were induced by sub-lethal treatment of SH-SY5Y cells with 500 μM hydrogen peroxide for 30 min. After H_2O_2 removal, mtDNA recovery was measured after 1, 2 and 48 h. As a result, we observed an initial MLF of 2.9 lesions per 10 kb mtDNA, followed by a significant repair of mitochondrial DNA after 1 h with a decrease of MLF from 2.4 to 1.0 in the second hour of regeneration. MtDNA damage was reversed almost entirely after 48 h (Figure 5C). Throughout the experiment, no morphological changes as well as no cell detachment could be observed indicating that the apparent mtDNA recovery was not caused by a separation of cells containing severely disrupted mtDNA molecules (data not shown). Moreover, LDH release, as a measure of cytotoxicity, was very moderate under these conditions. We further explored the impact of H_2O_2 derived mtDNA damage on mtDNA replication during the recovery process. By comparing the relative amount of mtDNA to nuclear genomic DNA during ROS insult and recovery, we found that H_2O_2 treatment did not alter the mtDNA level. A total of 500 μM hydrogen peroxide for 30 min had no stimulating effect on mtDNA synthesis in our experimental setting (Figure 5D). Interestingly, the relative number of mtDNA molecules decreased during the process of recovery supporting the hypothesis that severely damaged mtDNA is being degraded while less damaged mtDNA undergoes repair. Beyond the applicability to quantify mtDNA damage after exposure to different types of ROS, the SLR rt-PCR method has also been used successfully to monitor mtDNA recovery.

DISCUSSION

Up to the present, mitochondrial as well as nuclear DNA damage can be detected by a broad spectrum of methodically different approaches. One of the most prominent and widely used methods is Southern blot analysis, which is able to detect DNA strand breaks semi quantitatively via a multi-step procedure and requires high amounts of sample material (32,33). Single Cell Gel Electrophoresis, commonly known as comet assay, allows to detect single-and double-strand breaks as well as alkali-labile DNA sites under alkaline conditions (34,35), but these techniques deliver only partially quantifiable values.

Merely, high-performance liquid chromatography (HPLC) in combination with different detection methods, e.g. electrochemical (ECD) (36) or the recently described isotope dilution and tandem mass spectrometry (MS) (37) display a quantitative approach to detect specifically damaged DNA products. Hereby, the procedure relies on the liquid chromatographically purification of individual nucleosides followed by the separately quantification of alkylated, deaminated and oxidized DNA products by isotope-dilution and electrospray ionization LC/MS-MS (37). Subjected to its experimental settings, this method might also be applied to ROS derived DNA damage products, like 8-oxoguanine (8-oxoG) or abasic sites, but requires 4–6 d to complete depending on the number of samples and reflects only a partial status of damaged genomic sequences. In summary, all these techniques are tedious, involve radioactive labelling, or require

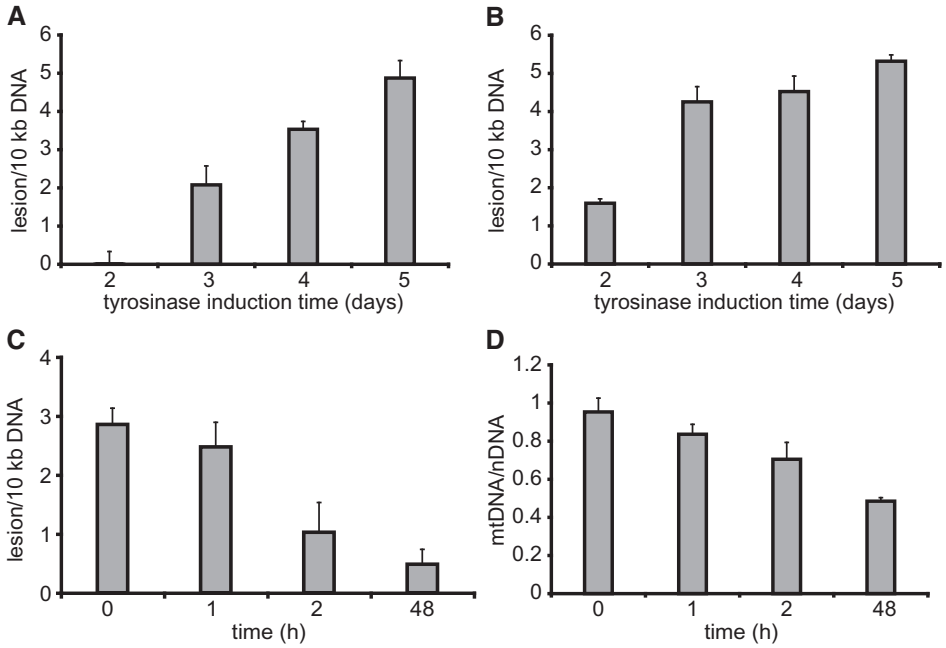

Figure 5. Tyrosinase overexpression induced differential mtDNA damage in coding regions (**A**) and in the non-coding D-Loop (**B**). Mitochondrial DNA recovery after H_2O_2-induced damage (**C**). TR8TY8 cells expressing Tyrosinase in presence of doxycycline for 0, 2, 3, 4 and 5 days exhibit tyrosinase-dependent exaltation of mtDNA impairment. Consistent with H_2O_2-induced damage, the DNA lesion rate is higher in the D-Loop (B) than in the four tested coding mtDNA sequences at all tested time points. ND1/2 region (A) represents damage rate similar to the other tested coding regions (ND4/5, COII/ATPase6/8, data not shown). (C) For mtDNA recovery, SH-SY5Y cells were treated with 500 μM H_2O_2 for 30 min followed by media replacement. Lesions in the mtDNA were detected by SLR rt-PCR directly after the oxidative insult and following DNA recovery. Lesion frequency was calculated using the $\Delta 2C_t$ method and expressed as relative DNA lesion rate. (**D**) In parallel, the mitochondrial copy number was determined by amplification of two mtDNA fragments which were normalized using two nuclear sequences. For each experimental condition rt-PCR was conducted in quadruplicates and the resulting average of C_p values for each fragment were used for data analysis. One nDNA fragment served as a normalisation control to calculate mtDNA copy number variation and non-treated cells were used as reference sample. The difference in the crossing point ΔC_p of untreated versus each treated condition of the nDNA reference fragment and each mtDNA fragment were calculated by the $2^{-\Delta\Delta CT}$ method expressed as ratio of mtDNA:nDNA for each mtDNA fragment individually to verify inter mtDNA copy number variation. Error bars designate standard deviation (at least three independent experiments).

considerable optimization efforts and a high amount of genomic DNA.

In the present work, we have successfully established a new and rapid Semi Long Run rt-PCR based assay for measuring mtDNA damage by detecting the inhibition of polymerase driven nucleotide amplification within a few hours. The method was validated to quantify mtDNA damage mediated directly by reactive oxygen species or by cellular consequences of the exposure to reactive oxygen species. In addition, the assay enabled us to monitor mtDNA repair kinetics by measuring recovery of amplification after removal of DNA damaging agents. Although, the majority of genomic lesions will be detected with high efficiency using our method, quantitative PCR-based approaches exhibit limited perceptibility for 8-hydroxydeoxyguanosine (8-OHdG) lesions that do not interfere entirely with DNA polymerase progression or primer annealing. However, oxidative stress is thought to generate a broad spectrum of different types of lesions and only a minor proportion of H_2O_2-induced lesions consists of 8-OHdG (38). Through the application of sequence-specific primers, our method permits the investigation of putative hot spots for mtDNA vulnerability along the mitochondrial genome and enables to study any genomic region of 1 kb size in the mitochondria as well as in the nucleus in a real-time approach.

The mitochondrial genome is known to be a more fragile target than nuclear DNA for endogenous and exogenous genotoxic insults. Heteroplasmic as well as homoplasmic somatic mtDNA mutations were identified in cells and tissues associated with a broad spectrum of cancer types and age-related diseases (for review see mitomap.org). Interestingly, DNA mutations are localised almost along the entire mitochondrial genome but predominantly in the non-coding regulatory D-Loop suggesting an increased susceptibility for somatic mutations in human cancer (39). Employing the SLR rt-PCR method, we were able to show that the D-Loop is indeed more prone to ROS derived DNA damage than other mtDNA loci. Although the reasons for this differential mtDNA damage remains cryptic, the unique, partially triple-stranded displaced structure in the D-Loop could be an explanation for the predisposition of this region to excessive DNA damaging.

Interestingly, the accumulation of mitochondrial nucleotide alterations and the destabilization of mtDNA has been described in the context of various diseases such as cancer (40) and several neurodegenerative disorders (41). In addition to the ageing process, persistent exposure to endogenous and environmental insults (e.g. UV radiation, smoking, alcohol) resulting in mitochondrial ROS and free radical generation steadily

increases the vulnerability of the mitochondrial genome (42–45), which impairs mitochondrial energy metabolism and finally leads to mitochondrial dysfunction and apoptosis. For maintaining cellular vitality, it is of prime importance to intercept the vicious circle (ROS formation ↔ impaired oxidative phosphorylation ↔ mtDNA damage) and to stimulate mitochondrial biogenesis. D-Loop formation is known to be an important structural characteristic for mtDNA replication initiation. Strikingly, MPP^+, a well known inhibitor of complex I of the mitochondrial respiratory chain and a PD-causative toxin was shown to specifically destabilize the D-Loop structure which resulted in an inhibition of mtDNA replication (46,47). In compliance, point mutations located close-by the replication origin in the D-Loop were associated with impairment of mitochondrial biogenesis in different types of cancer (48). In our study, following treatment with low H_2O_2 concentrations (100 μM and 200 μM), we found a higher degree of DNA damage in the mitochondrial D-Loop than in all other mtDNA sequences tested, emphasizing the higher sensitivity of the D-Loop region towards DNA damaging agents.

Monitoring the mtDNA recovery after H_2O_2 treatment, we found the initial mtDNA damage almost reversed after 48 h while the mtDNA copy number is reduced to 50%. These results indicate that mtDNA recovery might be a dynamic process of mtDNA repair, replication of undamaged or repaired mtDNA molecules, and degradation of affected mtDNA molecules depending on the level of DNA damage. It should be noted that the determination of mtDNA repair and copy number might be influenced by replication of nuclear DNA at late time points during the recovery process. A dilution effect caused by the increase of the rather undamaged nuclear DNA should be taken into account for the interpretation of those data. Through the application of different cellular stressors at various concentrations our method may provide a potential tool to identify the mechanisms that either lead to mitochondrial recovery or dysfunction.

In line with the quantitative PCR method of Santos and co-workers (22), our method allows to measure mtDNA damage and recovery but requires only three major steps (DNA isolation, SLR rt-PCR and data analysis) to complete the experiment. Importantly, it allows gene-specific analysis of mtDNA damage due to the short sequence of its experimental probes.

Laboratories investigating mitochondrial as well as nuclear genomic integrity and particularly scientists interested in research areas ranging from human and environmental bio-monitoring over DNA repair processes to genetic toxicology will greatly benefit from this new SLR rt-PCR method, which provides a quick and accurate tool to quantify DNA damage as well as mtDNA repair kinetics. Our technique qualifies as a screening method for the validation of mtDNA protecting and mitochondrial viability enhancing therapeutics in various diseases.

SUPPLEMENTARY DATA

Supplementary Data are available at NAR Online.

FUNDING

University of Tübingen, Fortüne-Grant F.1313010.2.

Conflict of interest statement. None declared.

REFERENCES

1. Mandavilli,B.S., Santos,J.H. and Van Houten,B. (2002) Mitochondrial DNA repair and aging. *Mut. Res.*, **509**, 127–151.
2. Kang,D. and Hamasaki,N. (2003) Mitochondrial oxidative stress and mitochondrial DNA. *Clin. Chem. Lab. Med.*, **41**, 1281–1288.
3. Valko,M., Izakovic,M., Mazur,M., Rhodes,C.J. and Telser,J. (2004) Role of oxygen radicals in DNA damage and cancer incidence. *Mol. Cell. Biochem.*, **266**, 37–56.
4. Yakes,F.M. and Van Houten,B. (1997) Mitochondrial DNA damage is more extensive and persists longer than nuclear DNA damage in human cells following oxidative stress. *Proc. Natl Acad. Sci. USA*, **94**, 514–519.
5. Yang,J.L., Weissman,L., Bohr,V.A. and Mattson,M.P. (2008) Mitochondrial DNA damage and repair in neurodegenerative disorders. *DNA Repair*, **7**, 1110–1120.
6. Kruman.II, Wersto,R.P., Cardozo-Pelaez,F., Smilenov,L., Chan,S.L., Chrest,F.J., Emokpae,R. Jr, Gorospe,M. and Mattson,M.P. (2004) Cell cycle activation linked to neuronal cell death initiated by DNA damage. *Neuron*, **41**, 549–561.
7. Linnane,A.W., Marzuki,S., Ozawa,T. and Tanaka,M. (1989) Mitochondrial DNA mutations as an important contributor to ageing and degenerative diseases. *Lancet*, **1**, 642–645.
8. Berneburg,M., Kamenisch,Y. and Krutmann,J. (2006) Repair of mitochondrial DNA in aging and carcinogenesis. *Photochem. Photobiol. Sci.*, **5**, 190–198.
9. Chen,J.Z. and Kadlubar,F.F. (2004) Mitochondrial mutagenesis and oxidative stress in human prostate cancer. *J. Environ. Sci. Health*, **22**, 1–12.
10. Druzhyna,N.M., Wilson,G.L. and Ledoux,S.P. (2008) Mitochondrial DNA repair in aging and disease. *Mech. Ageing Dev.*, **129**, 383–390.
11. Reeve,A.K., Krishnan,K.J. and Turnbull,D.M. (2008) Age related mitochondrial degenerative disorders in humans. *Biotechnol. J.*, **3**, 750–756.
12. Mecocci,P., MacGarvey,U. and Beal,M.F. (1994) Oxidative damage to mitochondrial DNA is increased in Alzheimer's disease. *Ann. Neurol.*, **36**, 747–751.
13. Wang,J., Xiong,S., Xie,C., Markesbery,W.R. and Lovell,M.A. (2005) Increased oxidative damage in nuclear and mitochondrial DNA in Alzheimer's disease. *J. Neurochem.*, **93**, 953–962.
14. Lovell,M.A. and Markesbery,W.R. (2007) Oxidative DNA damage in mild cognitive impairment and late-stage Alzheimer's disease. *Nucleic Acids Res.*, **35**, 7497–7504.
15. Lin,M.T. and Beal,M.F. (2006) Mitochondrial dysfunction and oxidative stress in neurodegenerative diseases. *Nature*, **443**, 787–795.
16. Schapira,A.H. (2008) Mitochondria in the aetiology and pathogenesis of Parkinson's disease. *Lancet Neurol.*, **7**, 97–109.
17. Bogdanov,M.B., Andreassen,O.A., Dedeoglu,A., Ferrante,R.J. and Beal,M.F. (2001) Increased oxidative damage to DNA in a transgenic mouse model of Huntington's disease. *J. Neurochem.*, **79**, 1246–1249.
18. Polidori,M.C., Mecocci,P., Browne,S.E., Senin,U. and Beal,M.F. (1999) Oxidative damage to mitochondrial DNA in Huntington's disease parietal cortex. *Neurosci. Lett.*, **272**, 53–56.
19. Bogdanov,M., Brown,R.H., Matson,W., Smart,R., Hayden,D., O'Donnell,H., Flint Beal,M. and Cudkowicz,M. (2000) Increased oxidative damage to DNA in ALS patients. *Free Radical Biol. Med.*, **29**, 652–658.

20. Warita,H., Hayashi,T., Murakami,T., Manabe,Y. and Abe,K. (2001) Oxidative damage to mitochondrial DNA in spinal motoneurons of transgenic ALS mice. *Brain Res.*, **89**, 147–152.
21. Van Houten,B., Woshner,V. and Santos,J.H. (2006) Role of mitochondrial DNA in toxic responses to oxidative stress. *DNA Repair*, **5**, 145–152.
22. Santos,J.H., Meyer,J.N., Mandavilli,B.S. and Van Houten,B. (2006) Quantitative PCR-based measurement of nuclear and mitochondrial DNA damage and repair in mammalian cells. *Methods Mol. Biol.*, **314**, 183–199.
23. Edwards,J.G. (2009) Quantification of mitochondrial DNA (mtDNA) damage and error rates by real-time QPCR. *Mitochondrion*, **9**, 31–35.
24. Sikorsky,J.A., Primerano,D.A., Fenger,T.W. and Denvir,J. (2007) DNA damage reduces Taq DNA polymerase fidelity and PCR amplification efficiency. *Biochem. Biophys. Res. Commun.*, **355**, 431–437.
25. Hasegawa,T., Matsuzaki,M., Takeda,A., Kikuchi,A., Furukawa,K., Shibahara,S. and Itoyama,Y. (2003) Increased dopamine and its metabolites in SH-SY5Y neuroblastoma cells that express tyrosinase. *J. Neurochem.*, **87**, 470–475.
26. Hasegawa,T., Treis,A., Patenge,N., Fiesel,F.C., Springer,W. and Kahle,P.J. (2008) Parkin protects against tyrosinase-mediated dopamine neurotoxicity by suppressing stress-activated protein kinase pathways. *J. Neurochem.*, **105**, 1700–1715.
27. Livak,K.J. and Schmittgen,T.D. (2001) Analysis of relative gene expression data using real-time quantitative PCR and the 2(-Delta Delta C(T)) Method. *Methods*, **25**, 402–408.
28. Ayala-Torres,S., Chen,Y., Svoboda,T., Rosenblatt,J. and Van Houten,B. (2000) Analysis of gene-specific DNA damage and repair using quantitative polymerase chain reaction. *Methods*, **22**, 135–147.
29. Kaufman,B.A., Durisic,N., Mativetsky,J.M., Costantino,S., Hancock,M.A., Grutter,P. and Shoubridge,E.A. (2007) The mitochondrial transcription factor TFAM coordinates the assembly of multiple DNA molecules into nucleoid-like structures. *Mol. Biol. Cell*, **18**, 3225–3236.
30. Takamatsu,C., Umeda,S., Ohsato,T., Ohno,T., Abe,Y., Fukuoh,A., Shinagawa,H., Hamasaki,N. and Kang,D. (2002) Regulation of mitochondrial D-loops by transcription factor A and single-stranded DNA-binding protein. *EMBO Rep.*, **3**, 451–456.
31. Heid,C.A., Stevens,J., Livak,K.J. and Williams,P.M. (1996) Real time quantitative PCR. *Genome Res.*, **6**, 986–994.
32. Southern,E.M. (1975) Detection of specific sequences among DNA fragments separated by gel electrophoresis. *J. Mol. Biol.*, **98**, 503–517.
33. Niwa,O. (2003) Induced genomic instability in irradiated germ cells and in the offspring; reconciling discrepancies among the human and animal studies. *Oncogene*, **22**, 7078–7086.
34. Tice,R.R., Agurell,E., Anderson,D., Burlinson,B., Hartmann,A., Kobayashi,H., Miyamae,Y., Rojas,E., Ryu,J.C. and Sasaki,Y.F. (2000) Single cell gel/comet assay: guidelines for in vitro and in vivo genetic toxicology testing. *Environ. Mol. Mut.*, **35**, 206–221.
35. Singh,N.P., McCoy,M.T., Tice,R.R. and Schneider,E.L. (1988) A simple technique for quantitation of low levels of DNA damage in individual cells. *Exp. cell Res.*, **175**, 184–191.
36. Kiyosawa,H., Suko,M., Okudaira,H., Murata,K., Miyamoto,T., Chung,M.H., Kasai,H. and Nishimura,S. (1990) Cigarette smoking induces formation of 8-hydroxydeoxyguanosine, one of the oxidative DNA damages in human peripheral leukocytes. *Free Radical Res. Commun.*, **11**, 23–27.
37. Taghizadeh,K., McFaline,J.L., Pang,B., Sullivan,M., Dong,M., Plummer,E. and Dedon,P.C. (2008) Quantification of DNA damage products resulting from deamination, oxidation and reaction with products of lipid peroxidation by liquid chromatography isotope dilution tandem mass spectrometry. *Nat. Protocols*, **3**, 1287–1298.
38. Termini,J. (2000) Hydroperoxide-induced DNA damage and mutations. *Mut. Res.*, **450**, 107–124.
39. Mambo,E., Gao,X., Cohen,Y., Guo,Z., Talalay,P. and Sidransky,D. (2003) Electrophile and oxidant damage of mitochondrial DNA leading to rapid evolution of homoplasmic mutations. *Proc. Natl Acad. Sci. USA*, **100**, 1838–1843.
40. Lee,H.C. and Wei,Y.H. (2009) Mitochondrial DNA instability and metabolic shift in human cancers. *Int. J. Mol. Sci.*, **10**, 674–701.
41. Schon,E.A. and Manfredi,G. (2003) Neuronal degeneration and mitochondrial dysfunction. *J. Clin. Invest.*, **111**, 303–312.
42. Fahn,H.J., Wang,L.S., Kao,S.H., Chang,S.C., Huang,M.H. and Wei,Y.H. (1998) Smoking-associated mitochondrial DNA mutations and lipid peroxidation in human lung tissues. *Am. J. Resp. Cell Mol. Biol.*, **19**, 901–909.
43. Mansouri,A., Fromenty,B., Berson,A., Robin,M.A., Grimbert,S., Beaugrand,M., Erlinger,S. and Pessayre,D. (1997) Multiple hepatic mitochondrial DNA deletions suggest premature oxidative aging in alcoholic patients. *J. Hepatol.*, **27**, 96–102.
44. Yang,J.H., Lee,H.C. and Wei,Y.H. (1995) Photoageing-associated mitochondrial DNA length mutations in human skin. *Arch. Dermatol. Res.*, **287**, 641–648.
45. Wei,Y.H. and Lee,H.C. (2002) Oxidative stress, mitochondrial DNA mutation, and impairment of antioxidant enzymes in aging. *Exp. Biol. Med.*, **227**, 671–682.
46. Umeda,S., Muta,T., Ohsato,T., Takamatsu,C., Hamasaki,N. and Kang,D. (2000) The D-loop structure of human mtDNA is destabilized directly by 1-methyl-4-phenylpyridinium ion (MPP+), a parkinsonism-causing toxin. *Eur. J. Biochem./FEBS*, **267**, 200–206.
47. Miyako,K., Irie,T., Muta,T., Umeda,S., Kai,Y., Fujiwara,T., Takeshige,K. and Kang,D. (1999) 1-Methyl-4-phenylpyridinium ion (MPP+) selectively inhibits the replication of mitochondrial DNA. *Eur. J. Biochem./FEBS*, **259**, 412–418.
48. Lee,H.C., Yin,P.H., Lin,J.C., Wu,C.C., Chen,C.Y., Wu,C.W., Chi,C.W., Tam,T.N. and Wei,Y.H. (2005) Mitochondrial genome instability and mtDNA depletion in human cancers. *Ann. NY Acad. Sci.*, **1042**, 109–122.